Modulating Functional Loop Movements: The Role of Highly Conserved Residues in the Correlated Loop Motions

Kannan Gunasekaran[a] and Ruth Nussinov*[a, b]

Loop flexibility in enzymes plays a vital role in correctly positioning catalytically important residues. This strong relationship between enzyme flexibility and function provides an opportunity to engineer new substrates and inhibitors. It further allows the design of site-directed mutagenesis experiments to explore enzymatic activity through the control of flexibility of a functional loop. Earlier, we described a novel mechanism in which a small loop triggers the motions of a functional loop in three enzymes (β-1,4-galactosyltransferase, lipase, and enolase) unrelated in sequence, structure, or function. Here, we further address the question of how the interactions between various flexible loops modulate the movements of the functional loop. We examine β-1,4-galactosyltransferase as a model system in which a Long loop undergoes a large conformational change (moves in space up to 20 Å) upon substrate binding in addition to a small loop (Trp loop) that shows a considerably smaller conformational change. Our molecular-dynamics simulations carried out in implicit and explicit solvent show that, in addition to these two loops, two other neighboring loops are also highly flexible. These loops are in contact with either the Long loop or the Trp loop. Analysis of the covariance of the spatial displacement of the residues reveals that coupled motions occur only in one of these two loops. Sequence analysis indicates that loops correlated in their motions also have highly conserved residues involved in the loop – loop interactions. Further, analysis of crystal structures and simulations in explicit water open the possibility that the Trp loop that triggers the movement of the Long loop in the unbound conformation may also play the same role in the substrate-bound conformation through its contact with the conserved and correlated third loop. Our proposition is supported by the observation that four of the five conserved positions in the third loop are at the interface with the Trp loop. Evolution appears to select residues that drive the functional Long loop to a large conformational change. These observations suggest that altering selected loop – loop interactions might modulate the movements of the functional loop.

Introduction

Protein motions range from simple bending and stretching of bonds to subunit rotations and translations.[1] Conformational changes associated with loop(s) are critically important for enzyme function.[2] Several experimental and theoretical studies have shown that flexibility is an integral part of protein function (Scheme 1).[3] Understanding how protein motions control enzyme catalysis is fundamental to drug discovery.[4] Well-studied examples include protein kinases, triosephosphate isomerase, fructose-1,6-bisphosphate aldolase, HIV protease, lipase, and enolase.[5] Recently, β-1,4-galactosyltransferase (β4Gal-T1) has been shown to undergo a large conformational change to create binding sites for oligosaccharides and α-lactalbumin.[6] β4Gal-T1 is a 402-residue-long enzyme that catalyzes the transfer of galactose from UDP-galactose (UDP-Gal) to *N*-acetylglucosamine. It also forms a 1:1 complex with α-lactalbumin to synthesize lactose. Comparison of the crystal structures of the enzyme with the substrate bound and unbound reveals a large conformational change (displacement of up to 20 Å) in a Long loop comprising residues Ile345 to His365.[6a] Another loop that has a conserved Trp residue (Trp314) flanked by multiple glycine residues undergoes a relatively smaller conformational change (Tyr311 to Gly316; Trp loop). Both molecular-dynamics simulations and limited proteolysis experiments have confirmed the flexibility associated with the Long loop in solution.[7] Multiple implicit-solvent as well as explicit-solvent simulations carried out on this enzyme have also revealed that the conformational change associated with the Long loop is triggered by the Trp loop. In the absence of contacts between the Trp and the Long loops, the energy barrier for the transition of the Long loop from the unbound to the bound state is higher. The increase in the energy is estimated by using implicit-solvent simulations to vary from 28 to 61 kcal mol^{-1}, and with explicit-water simulations to be around 45 kcal mol^{-1}. The simulations have also shown that mutation of

[a] *Dr. K. Gunasekaran, Prof. R. Nussinov*
Basic Research Program, SAIC-Frederick, Inc.
Laboratory of Experimental and Computational Biology
NCI-Frederick, building 469, room 151
Frederick, MD 21702 (USA)
Fax: (+1) 301-846-5598
E-mail: ruthn@ncifcrf.gov

[b] *Prof. R. Nussinov*
Sackler Institute of Molecular Medicine
Department of Human Genetics and Molecular Medicine
Sackler School of Medicine, Tel Aviv University
69978 Tel Aviv (Israel)

  DOI: 10.1002/cbic.200300732

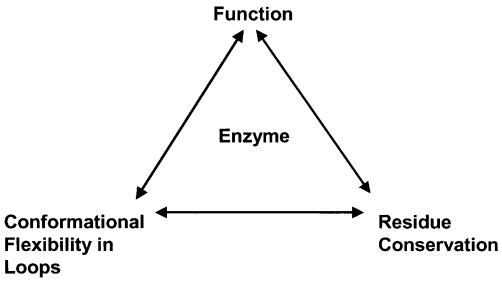

Scheme 1. *Conformational flexibility in loops is critical for enzyme function. Thus, we may expect that there would be an evolutionary pressure to conserve residues that are critical for loop flexibility. For our case here, we first identified loops that displayed correlated motions. We were able to derive the sequence of events from the open to the closed conformation, and have hints for the path from the closed to the open. We proceeded to pinpoint the critical residues involved in the loop – loop interactions. Next, we carry out a conservation study using the sequence database. We found consistency between the residues identified as critical in the molecular-dynamics simulation and in the sequence database conservation analysis. The identified residues may provide an opportunity to design or modulate function through control of flexibility.*

the glycine residues in the Trp loop to alanine, restraining the Trp loop, or repositioning the Trp loop (such that it does not make any contact with the Long loop) all had dramatic effects on the movement of the Long loop. Importantly, as predicted by the simulations, when the Trp314Ala mutant was crystallized in the unbound conformation, the Long loop conformation was significantly affected.[6d] The mutant also showed a significant loss in its catalytic activity. These findings have indicated that the Trp loop triggers the movement of the Long loop. In our earlier study, in addition to β4Gal-T1, we also observed a triggering loop mechanism in two other enzymes: lipase and enolase. These three enzymes differ in sequence, folding, and function. Combined, these findings have led us to conclude that evolution has modulated and adapted essentially the same mechanism for different types of functions.[7] We speculated that evolution might conserve and repeatedly utilize skillful mechanisms: A particular function modulates and adapts a general "skillful" mechanism to a specific enzymatic reaction.

Here, we use molecular-dynamics simulations to examine all flexible regions in β4Gal-T1. We address the question of how the interactions between various flexible loops modulate the movements of the functional loop (Long loop) in the substrate-bound and -unbound conformations. We carried out covariance analysis of the spatial displacement of residues in order to identify loops that show correlated movements with the functional loop. Our analysis reveals that selective loop – loop interactions play a role in modulating the movement of the functional loop. Interestingly, loops coupled in motions also have highly conserved residues involved in the loop – loop interactions. The observations indicate that the movement of the Long loop from the bound to the unbound state could also be triggered by the Trp loop, as in the case of the unbound to the bound state. The correlated motions, conserved by evolution, illustrate an elegant mechanism. Our results are consistent with recent observations on dihydrofolate reductase, in which molecular-dynamics simulations revealed coupled motions between loops,[8a, b] and sequence analysis indicated that conserved residues could play a role in the network of coupled motions.[8c] β4Gal-T1 provides a unique opportunity to examine the mechanism of loop movements since it undergoes a large conformational change and multiple loops are involved.

Results and Discussion

Comparison of the substrate bound and unbound enzyme crystal structures reveals that two regions undergo conformational changes in β4Gal-T1: a) a Long loop comprising residues Ile345 to His365, and b) a small loop from Tyr311 to Gly316 containing a catalytically important tryptophan residue (Trp loop; Figure 1 a). A series of 10 ns implicit-solvent molecular-dynamics (MD) simulations at 300 K carried out earlier and in this work on the unbound structure reveals that, in addition to the Long loop (functional loop) and the Trp loop, two other loops also show high backbone root-mean-squared deviations (RMSD) indicating conformational flexibility: Gln220 to Lys230 (Loop 1) and Val275 to Val287 (Loop 2; Figure 1 b). However, Loops 1 and 2 do not show any structural variation when the substrate-bound and -unbound crystal structures are compared (Figure 1 a).

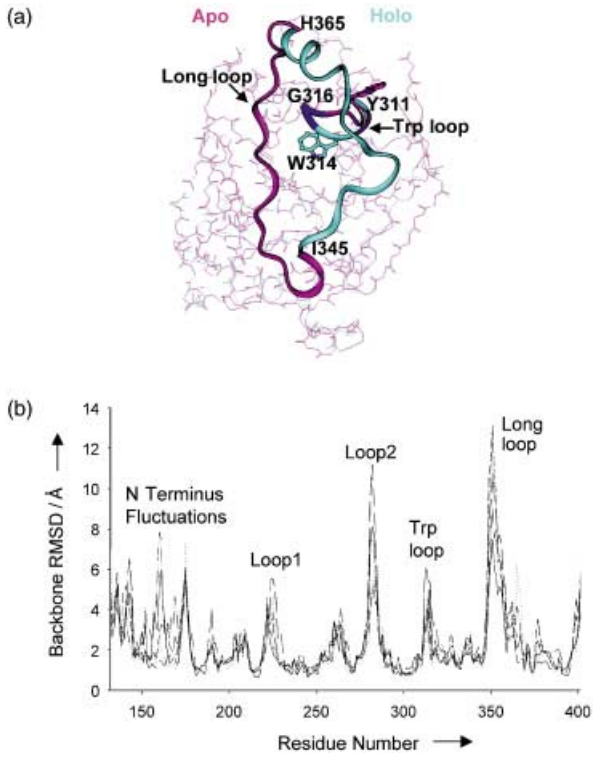

Figure 1. *a) C^{α} superposition of crystal structures of β4Gal-T1 crystallized without (purple, unbound; 2.4 Å resolution) and with (cyan, bound; 2.0 Å resolution) the substrate UDP-Gal. A significant structural change is seen in a Long loop (Ile345 to His365) and in a short loop (Trp loop: Tyr311 to Gly316) containing a tryptophan residue (Trp314). The Long loop's position moves as far as 20 Å between the unbound and bound conformations. b) Residue-wise backbone root-mean-squared deviations (RMSD) calculated from the five 10 ns implicit-solvent molecular-dynamics simulations at 300 K. Apart from the N terminus, a total of four loops show high fluctuations.*

In the substrate unbound crystal structure, Loop 1 is positioned adjacent to the Trp loop and is involved in side chain – side chain as well as backbone – side chain interactions with the Trp loop. In particular, there is a hydrogen-bonding interaction between Asn227 and Asn309. In the substrate-bound conformation, Loop 1 also interacts with the Long loop and possibly plays a role in stabilization. Loop 2 is placed adjacent to the Long loop, and some of the Long-loop residues interact with Loop 2. In particular, Asn353 is involved in side chain – backbone hydrogen bonding interaction with Gly281, and there is also a backbone – backbone hydrogen bonding interaction between Glu354 and Lys279.

During the 10 ns implicit-solvent simulations, the Long loop quickly (within 2 ns) moves to an intermediate position between the unbound and bound conformations and remains stable at this position for the remaining 8 ns of the simulation. The Trp loop moves in the opposite direction, making several hydrophobic and hydrogen-bonding interactions with the Long-loop residues. A set of 4 ns explicit-water simulations on β4Gal-T1 confirms these observations. As can be seen in Figure 2a, Loop 1 and Loop 2 do not show large positional displacement as compared to the Trp and Long loops. We further examined the stability of the protein and convergence of our simulations through analysis of RMSD versus duration of the simulations (Figure 2b). Figures 1b and 2b show that, apart from the identified loops and the N terminus, the core of the protein remains stable. Further, Figure 2b shows that there is no significant increase in the RMSD value after 2.0 ns; this indicates that the simulation samples stable conformations.

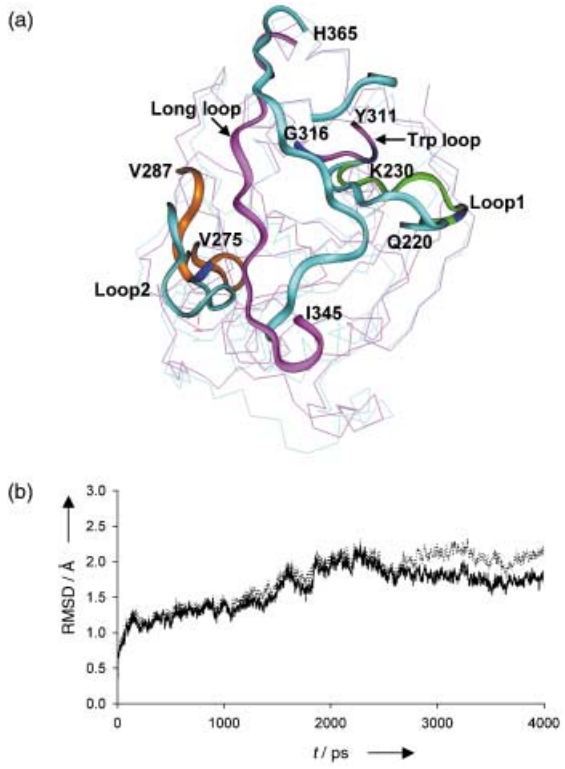

Figure 2. *a) Cα superposition of the starting structure (purple, unbound) and a snapshot of β4Gal-T1 (cyan) observed during a 4 ns explicit-water simulation at 300 K. The identified flexible loops are shown in ribbon model. Loop 1 (green in the starting structure) and Loop 2 (brown) show much less structural deviation than the Trp and Long loops. The glycine positions in the loops are shown in blue in the starting structure. b) Plot of RMSD versus time, calculated based on Cα positions between equilibrated crystal structure (unbound) and snapshots observed in the simulations. The dotted line represents the entire structure, while the solid line is without considering the N terminus (Thr132 – Pro179) and the Long loop (Ile345 – His365). The RMSD value remains stable at around 1.8 Å after 2.0 ns simulations, this indicates sampling of stable conformations. It may be noted here that in addition to the N terminus and the Long loop, there are also other loops that undergo significant fluctuations as shown in Figure 1b.*

In order to address the question of whether the spatial displacements of the identified flexible loops are correlated during the 4 ns explicit-water simulations, we carried out a covariance analysis. The covariance of the spatial displacement of the residues was calculated based on Cα positions by using X-PLOR (Figure 3). A covariance value of 1 would indicate that the motions are coupled while a value of 0 would indicate that there is no correlation. High correlation is seen among the Trp loop, Long loop, and Loop 1. Although the Long loop and Loop 1 are not in contact in the unbound crystal structure, the coupled motions between the two may arise through the contacts of Loop 1 with the Trp loop, which in turn makes contact with the Long loop (Figure 4). Further, Loop 1 makes contact with the Long loop in the substrate-bound conformation. Thus, Loop 1 is likely to further drive and stabilize the Long loop in its substrate-bound conformation. It is also possible that the Trp loop, which triggers the movement of the Long loop in the substrate-unbound conformation, may also play the same role in the substrate-bound conformation. The Trp loop may trigger the

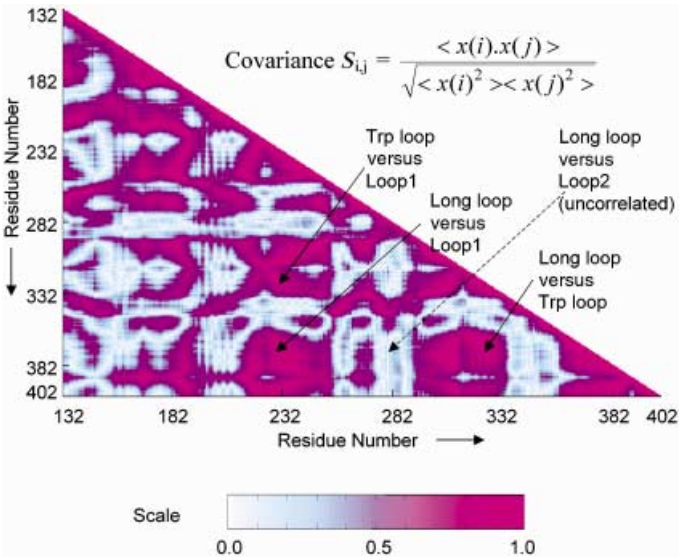

Figure 3. *The covariance matrix plot calculated from 4 ns explicit-water simulations on β4Gal-T1 unbound conformation by using X-PLOR.[13] The covariance ($S_{i,j}$) of the spatial displacements of two Cα atoms, i and j, was calculated by using the formula shown in the figure, where x[i] and x[j] are the coordinate displacements relative to the average positions of atom i and j. As can be seen from the figure, the Long-loop movement is correlated with the Trp loop and Loop 1, while it is uncorrelated with the Loop 2 (although, Loop 2 shows high fluctuations during the implicit- and explicit-water simulations and is in contact with the Long loop in the unbound crystal structure).*

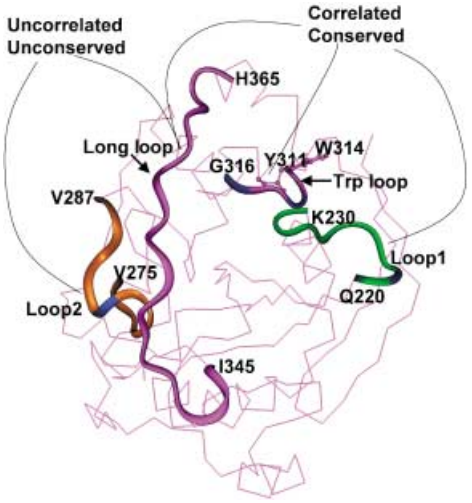

Figure 4. *β4Gal-T1 with all the identified flexible loops shown in ribbon model. The Long loop is correlated with the Trp loop and Loop 1. Although the Long loop and Loop 2 are neighbors, their movements are not correlated. Analysis of the PFAM database shows that the interactions between the Loop 1, Trp, and the Long loop involve highly conserved residues. The glycine positions in the loops are in blue.*

movement of the Long loop in the bound conformation through its contact with Loop 1, which in turns makes contact with the Long loop. Interestingly, although Loop 2 is involved in backbone – backbone as well as sidechain – sidechain interactions with the Long loop, its movements are not coupled with those of the Long loop.

We also searched the Protein families database of alignment (PFAM) for highly conserved (> 80 %) positions in the identified flexible loops.[9] The consistency between the conserved positions and the coupled loops is striking. Our earlier analysis showed that residues involved in the interactions between the Long loop and the Trp loop are highly conserved (Figure 5).[7] In the present work, we note that this is also the case for the Trp loop and Loop 1. The Phe226, Asn227, Arg228, and Ala229 positions in Loop 1 are highly conserved in the β4Gal-T1 family (Figure 6). Similarly, residues in the Trp loop are also highly conserved. Again, both loops are also coupled in their motions. In the unbound crystal structure, Asn227 $N^{\delta 2}$ is hydrogen bonded to the Asn309 backbone oxygen atom, and Ala229 C^{β} is in contact (distance < 4.5 Å) with Pro308 C^{γ}, and, in the bound conformation, Phe226 C^{β} is in contact with Asn353 C^{β}. In the energy-minimized unbound structure, Arg228 is involved in the side chain – side chain hydrogen bonding interaction with Glu317. Figure 7a shows that conserved positions in Loop 1 are at the interface with the Trp loop. Of the five highly conserved positions, four are at the interface with the Trp loop. This further supports the proposition that the conserved residues promote coupled motions.

Interestingly, in contrast to the Trp loop and the Loop 1 case, no conserved position is involved in the interaction between the Long loop and Loop 2. Leu284 and Tyr286 are the only two positions that show conservation in Loop 2 (Figure 6). Remarkably, both positions point away from the Long loop and do not

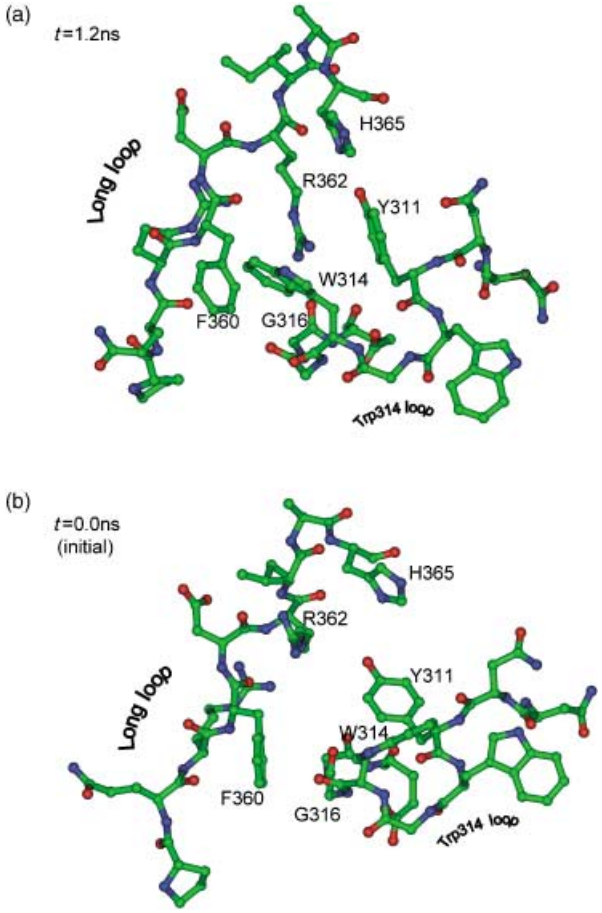

Figure 5. *Interactions between the Long and Trp loops during a 4 ns explicit-water simulations on the unbound conformation of β4Gal-T1. The residues involved in the interactions are highly conserved in the β4Gal-T1 family.[7] a) Snapshot of the interactions observed at 1.2 ns; b) positions in the starting conformation (t = 0), for comparison.*

interact with it even during the molecular dynamics simulations (Figure 7). We also examined the possibility that the interacting residues in these two loops could undergo correlated mutations (and thus a single position may not show conservation);[10] however, we did not find any such examples. These observations are consistent with the covariance analysis, in which we did not see any coupling between the motions of the Long loop and Loop 2. It is also interesting to note that the correlated movement occurs in the direction of the Long loop movement toward its substrate-bound conformation.

Conclusion

Understanding how protein motions control enzyme catalysis has broad implications in the design of new substrates and inhibitors.[4] Further, such an understanding could be useful in the design of site-directed-mutagenesis experiments to investigate enzymatic reactions. The work presented here suggests that modifying the interactions between the functional loop and its neighbors, whose motions are coupled, could alter the functional-loop movements. The study also suggests that only

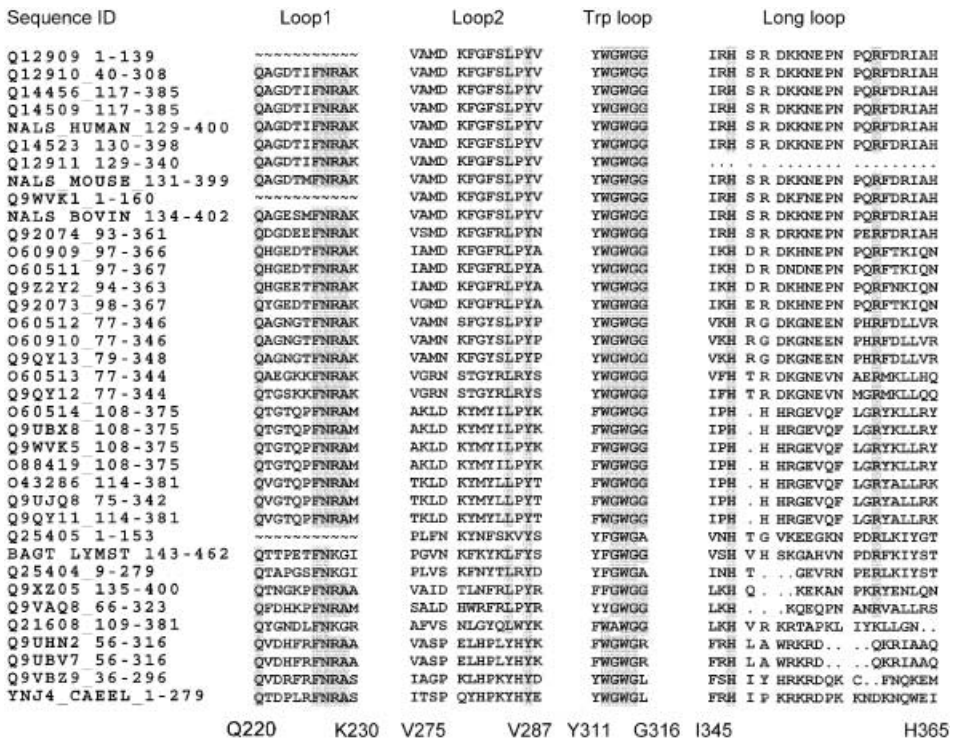

Figure 6. *Sequence alignment of 37 members of the β4Gal-T1 family (alignment taken from the PFAM database[9]). The alignment is shown for the segments corresponding to the four identified flexible loops (Figure 1 b). Loop 2 has only two conserved positions, both point away from the Long loop. On the other hand, many of the Loop 1 residues are highly conserved and are involved in interactions with the Trp loop. The Trp loop sequence is also highly conserved in the β4Gal-T1 family. The positions conserved in more than 80% of the sequences are shaded in gray.*

some loops play a role in modulating function by controlling the movement of the functional loop. Since not all of the loops that are neighbors of the functional loop show coupled motions, molecular-dynamics simulations appear to be a useful technique for identifying those loops involved in correlated movements.

Interestingly, in the example studied here (β4Gal-T1), loops with correlated movements also show significant conservation of amino acids involved in loop – loop interactions. The consistency between the correlated loops (as identified by explicit-water simulations) and the conserved interactions (as identified from the PFAM database) is striking. A comparison of the substrate-unbound and -bound β4Gal-T1 crystal structures reveals that the Long and the Trp loops show conformational variations. However, during the simulation, two additional loops (Loops 1 and 2) also exhibit flexibility. Examination of the covariance of the spatial displacements of these four loops reveals, that of the four loops that show high flexibility during the simulations, only three display correlated movements. Although in the substrate-unbound crystal structure Loop 2 and the Long loop are in contact, their movements are not coupled. Consistently, residues involved in the interactions between the Long loop and Loop 2 are not conserved either. Loop 1 is located away from the Long loop in the substrate-unbound conformation; however, they are coupled in their motions. The coupled motions could occur through the interactions of Loop 1 with the Trp loop. Consistently, residues involved in the interactions between the Trp loop and Loop 1 are also highly conserved. Both hydrogen-bonding and hydrophobic interactions are observed to play a role in the loop – loop interactions. This could suggest that evolution preserved these residues in order to modulate the movements of the functional loop.

To conclude, the motions of Loop 1 are coupled with those of the Trp loop. The motions of the Trp loop are in turn coupled with those of the Long loop. The Trp loop triggers the closure of the functional Long loop from the unbound to the bound state. It appears that the movement of the Long loop from the bound to the unbound state is also triggered by the Trp loop. However, it is triggered through Loop 1. The correlated motions, conserved by evolution, illustrate an elegant mechanism. Earlier we observed a similar closure mechanism in three unrelated enzymes, β4Gal-T1, lipase, and enolase. It is yet to be investigated if the opening mechanism seen in β4Gal-T1 is also observed in the other two unrelated enzymes.

Computational Methods

We have considered the β4Gal-T1 segment comprised of residues Thr132 to Ser402, for which coordinates are available in both conformations (PDB code 1FGXA (apo), 1J8XB (holo)).[11] A set of five MD simulations in implicit solvent was carried out to explore the dynamic behavior of the β4Gal-T1. MD simulations in explicit water were also carried out in order to analyze the covariance of the loops. For the implicit-solvent simulations, we used the effective energy function (EEF1) combined with the CHARMM19 polar hydrogen potential energy function.[12] For the implicit-solvent simulation with the EEF1 forcefield, the crystal structures were subjected to 300 steps of minimization by using the adopted basis Newton – Raphson routine (ABNR) available in the CHARMM package (version c27b1). In the initial phase of heating, the simulation temperature was slowly raised in steps, with the system preserving the crystallographic structure. At the final required temperature (300 K), the system was equilibrated for 50 to 100 ps (10^{-12} s) with a time step of 2 fs (10^{-15} s). The equilibration period was followed by a longer duration of productive MD simulations with a time step of 2 fs. The SHAKE constraint on bond lengths within CHARMM was turned on. The conformers were saved at 2 ps intervals. In order to remove the center-of-mass motions, the saved conformers were superimposed on the minimized starting structure by using InsightII (Accelrys, Inc., San Diego). The structures were superimposed by considering either all backbone or all C^{α} atoms as needed. For the explicit-water

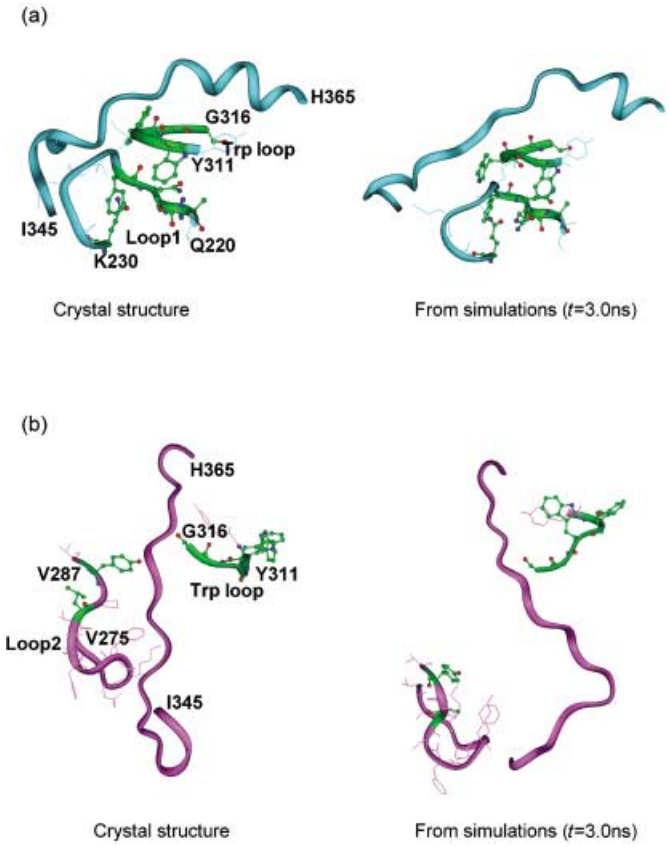

Figure 7. *Conserved positions in Loop 1, Loop 2, and the Trp loop depicted on the substrate-bound (a) and -unbound (b) crystal and simulated structures. The highly conserved positions (>80%) are shown in ball-and-stick model with the backbone ribbon representation in green. In (a), of the five conserved positions in Loop 1, four are at the interface with the Trp loop. b) There are only two conserved positions in Loop 2, both are far from the Trp loop and do not interact with the Long loop even during the simulations. For reference, the Long loop is shown in ribbon representation.*

simulations on β4Gal-T1, in addition to the crystal structure, we also considered the associated crystal water. A total of 81 crystal water molecules were included for the unbound and 96 for the bound conformer. The systems were then soaked in a cubic water box with an edge length of 65 Å. Care was taken to ensure that the effective water density remained close to 1.0 g cm^{-3} (a total of 7608 water molecules were included). The systems were then subjected to minimization, followed by slow heating and equilibration before the productive runs. The periodic boundary condition was imposed so that a constant number of water molecules would be maintained during the simulations. The nonbonded interactions were truncated at 12.0 Å. A time step of 1 fs was used for the simulations, and the conformers were saved at an interval of 1 ps. When multiple simulations were required, the random seed, and the heating and equilibration periods were all manipulated in order to generate different trajectories.

Acknowledgements

We thank Drs. Buyong Ma, Chung-Jung Tsai, David Zanuy, Gavin Tsai, Pradman K. Qasba, Boopathy Ramakrishnan, and in particular Jacob V. Maizel for numerous helpful discussions. We thank the NCI-Frederick Advanced Biomedical Computing Center for time and assistance. This study utilized the high-performance computational capabilities of the Biowulf/LoBoS3 cluster at the National Institutes of Health, Bethesda, MD. The research of R.N. in Israel was supported in part by the "Center of Excellence in Geometric Computing and its Applications" funded by the Israel Science Foundation (administered by the Israel Academy of Sciences), by a Ministry of Science Grant, by an Adams Brain Center Grant, and by Tel Aviv University Basic Research Grants. This project has been funded in part with Federal funds from the National Cancer Institute, National Institutes of Health, under contract number NO1-CO-12400. The content of this publication does not necessarily reflect the view or policies of the Department of Health and Human Services, neither does mention of trade names, commercial products, or organization imply endorsement by the U.S. Government.

Keywords: conformation analysis · correlated motions · function design · ligand binding mechanism · proteins · transferases

[1] a) J. M. Yon, D. Perahia, C. Ghelis, *Biochimie* **1998**, *80*, 33 – 42; b) J. J. Falke, *Science* **2002**, *295*, 1480 – 1481; c) W. S. Bennett, R. Huber, *CRC Crit. Rev. Biochem.* **1984**, *15*, 291 – 384; d) G. G. Hammes, *Biochemistry* **2002**, *41*, 8221 – 8228; e) G. Weber, *Biochemistry* **1972**, *11*, 864 – 878.

[2] D. Joseph, G. A. Petsko, M. Karplus, *Science* **1990**, *249*, 1425 – 1428.

[3] a) A. J. Wand, *Nat. Struct. Biol.* **2001**, *8*, 926 – 931; b) A. Fontana, P. Polverino de Laureto, V. De Filippis, E. Scaramella, M. Zambonin in *Proteolytic Enzymes: Tools and Targets* (Eds.: E. E. Sterchi, W. Stocker), Springer, Heidelberg, **1999**, pp. 253 – 280; c) S. Doniach, P. Eastman, *Curr. Opin. Struct. Biol.* **1999**, *9*, 157 – 163; d) M. Karplus, J. A. McCammon, *Nat. Struct. Biol.* **2002**, *9*, 646 – 652; e) T. Hansson, C. Oostenbrink, W. F. van Gunsteren, *Curr. Opin. Struct. Biol.* **2002**, *12*, 190 – 196.

[4] a) T. A. Fritz, D. Tondi, J. S. Finer-Moore, M. P. Costi, R. M. Stroud, *Chem. Biol.* **2001**, *8*, 981 – 995; b) S. J. Teague, *Nat. Rev. Drug Discovery* **2003**, *2*, 527 – 541.

[5] a) L. K. Nicholson, T. Yamazaki, D. A. Torchia, S. Grzesiek, A. Bax, S. J. Stahl, J. D. Kaufman, P. T. Wingfield, P. Y. Lam, P. K. Jadhav, C. N. Hodge, P. J. Domaille, C.-H. Chang. *Nat. Struct. Biol.* **1995**, *2*, 274 – 280; b) L. Lebioda, B. Stec, J. M. Brewer, *J. Biol. Chem.* **1989**, *264*, 3685 – 3693; c) L. Lebioda, B. Stec, *Biochemistry* **1991**, *30*, 2817 – 2822; d) Z. S. Derewenda, *Adv. Protein Chem.* **1994**, *45*, 1 – 52; e) S. Zgiby, A. R. Plater, M. A. Bates, G. J. Thomson, A. Berry, *J. Mol. Biol.* **2002**, *315*, 131 – 140; f) M. Huse, J. Kuriyan *Cell* **2002**, *109*, 275 – 282; g) Y. Nagao, S. Kitada, K. Kojima, H. Toh, S. Kuhara, T. Ogishima, A. Ito, *J. Biol. Chem.* **2000**, *275*, 34552 – 34556.

[6] a) B. Ramakrishnan, P. K. Qasba, *J. Mol. Biol.* **2001**, *310*, 205 – 218; b) B. Ramakrishnan, P. V. Balaji, P. K. Qasba, *J. Mol. Biol.* **2002**, *318*, 491 – 502; c) L. N. Gastinel, C. Cambillau, Y. Bourne, *EMBO J.* **1999**, *18*, 3546 – 3557; d) V. Ramasamy, B. Ramakrishnan, E. Boeggeman, P. K. Qasba, *J. Mol. Biol.* **2003**, *331*, 1065 – 1076.

[7] a) K. Gunasekaran, B. Ma, B. Ramakrishnan, P. K. Qasba, R. Nussinov. *Biochemistry* **2003**, *42*, 3674 – 3687; b) K. Gunasekaran, B. Ma, R. Nussinov, *J. Mol. Biol.* **2003**, *332*, 143 – 159.

[8] a) J. L. Radkiewicz, C. L. Brooks III, *J. Am. Chem. Soc.* **2000**, *122*, 225 – 231; b) T. H. Rod, J. L. Radkiewicz, C. L. Brooks III, *Proc. Natl. Acad. Sci. USA* **2003**, *100*, 6980 – 6985; c) P. K. Agarwal, S. R. Billeter, P. T. R. Rajagopalan, S. J. Benkovic, S. Hammes-Schiffer. *Proc. Natl. Acad. Sci. USA* **2002**, *99*, 2794 – 2799.

[9] A. Bateman, E. Birney, L. Cerruti, R. Durbin, L. Etwiller, S. R. Eddy, S. Griffiths-Jones, K. L. Howe, M. Marshall, E. L. Sonnhammer, *Nucleic Acids Res.* **2002**, *30*, 276 – 280.

[10] a) L. Oliveira, A. C. Paiva, G. Vriend. *ChemBioChem* **2002**, 3, 1010 – 1017; b) K. Gunasekaran, A. T. Hagler, L. M. Gierasch. *Proteins: Struct. Funct. Genet.* **2004**, in press (published online on Sep. 4, **2003**; DOI: 10.1002/prot.10520; http://www3.interscience.wiley.com/cgi-bin/jhome/36176).

[11] F. C. Bernstein, T. F. Koetzle, G. J. Williams, E. F. Meyer, Jr., M. D. Brice, J. R. Rodgers, O. Kennard, T. Shimanouchi, M. Tasumi, *J. Mol. Biol.* **1977**, *112*, 535 – 542.

[12] a) B. R. Brooks, R. E. Bruccoleri, B. D. Olafson, D. J. States, S. Swaminathan, M. Karplus, *J. Comput. Chem.* **1983**, *4*, 187 – 217; b) T. Lazaridis, M. Karplus. *Proteins: Struct. Funct. Genet.* **1999**, *35*, 133 – 152.

[13] A. T. Brunger, X-PLOR, **1992**, Version 3.1. A system for X-ray crystallography and NMR. Yale University Press, New Haven.

Received: August 1, 2003 [F732]

